Available online at www.sciencedirect.com
SCIENCE DIRECT
Science of the Total Environment 368 (2006) 177–188
Science of the Total Environment
An International Journal for Scientific Research into the Environment and its Relationship with Humankind
www.elsevier.com/locate/scitotenv

Influences of iron, manganese, and dissolved organic carbon on the hypolimnetic cycling of amended mercury

Shawn P. Chadwick [a,*], Chris L. Babiarz [a], James P. Hurley [a,b], David E. Armstrong [a]

[a] University of Wisconsin-Madison, Environmental Chemistry and Technology Program, 660 North Park Street, Madison, WI 53706-1481, USA
[b] University of Wisconsin Aquatic Sciences Center, 1975 Willow Drive Madison, WI 53706-1177, USA

Received 15 October 2004; received in revised form 18 May 2005; accepted 12 September 2005
Available online 11 October 2005

Abstract

The biogeochemical cycling of iron, manganese, sulfide, and dissolved organic carbon were investigated to provide information on the transport and removal processes that control the bioavailability of isotopic mercury amended to a lake. Lake profiles showed a similar trend of hypolimnetic enrichment of Fe, Mn, DOC, sulfide, and the lake spike (^{202}Hg, purity 90.8%) and ambient of pools of total mercury (HgT) and methylmercury (MeHg). Hypolimnetic enrichment of Fe and Mn indicated that reductive mobilization occurred primarily at the sediment–water interface and that Fe and Mn oxides were abundant within the sediments prior to the onset of anoxia. A strong relationship ($r^2=0.986$, $n=15$, $p<0.001$) between filterable Fe and Mn indicated that reduction of Fe and Mn hydrous oxides in the sediments is a common in-lake source of Fe(II) and Mn(II) to the hypolimnion and that a consistent Mn : Fe mass ratio of 0.05 exists in the lake. A strong linear relationship of both the filterable [Fe] ($r^2=0.966$, $n=15$, $p<0.001$) and [Mn] ($r^2=0.964$, $n=15$, $p<0.001$) to [DOC] indicated a close linkage of the cycles of Fe and Mn to DOC. Persistence of iron oxides in anoxic environments suggested that DOC was being co-precipitated with Fe oxide and released into solution by the reductive dissolution of the oxide. The relationship between ambient and lake spike HgT ($r^2=0.920$, $n=27$, $p<0.001$) and MeHg ($r^2=0.967$, $n=23$, $p<0.001$) indicated that similar biogeochemical processes control the temporal and spatial distribution in the water column. The larger fraction of MeHg in the lake spike compared to the ambient pool in the hypolimnion suggests that lake spike may be more available for methylation. A linear relationship of DOC to both filterable ambient HgT ($r^2=0.406$, $n=27$, $p<0.001$) and lake spike HgT ($r^2=0.314$, $n=15$, $p=0.002$) suggest a role of organic matter in Hg transport and cycling. However, a weak relationship between the ambient and lake spike pools of MeHg to DOC indicated that other processes have a major role in controlling the abundance and distribution of MeHg. Our results suggest that Fe and Mn play important roles in the transport and cycling of ambient and spike HgT and MeHg in the hypolimnion, in part through processes linked to the formation and dissolution of organic matter-containing Fe and Mn hydrous oxides particles.
© 2005 Elsevier B.V. All rights reserved.

Keywords: METAALICUS; Mercury; Methylmercury; Cycling; Iron; DOC

1. Introduction

Speciation of mercury (Hg) plays an important role on the fate and transport of mercury in aquatic environments (Miskimmin et al., 1992; Watras et al., 1995; Babiarz et al., 1998; Benoit et al., 1999b) and its subsequent methylation (Compeau and Bartha, 1985;

* Corresponding author. Tel.: +1 608 658 5291; fax: +1 608 262 0454.
E-mail address: spchadwick@wisc.edu (S.P. Chadwick).

0048-9697/$ - see front matter © 2005 Elsevier B.V. All rights reserved.
doi:10.1016/j.scitotenv.2005.09.039

Gilmour et al., 1992; Benoit et al., 1999a, 2001a,b; Mehrotra et al., 2003). Detailed information regarding the chemical and physical speciation of Hg and methylmercury (MeHg) can help elucidate the transport and removal processes that control bioavailability of the Hg for methylation and bioaccumulation. The speciation of Hg and MeHg is hypothesized to be controlled by organic and inorganic aqueous-phase speciation (e.g., sulfide, thiol-containing DOM) and solid-phase partitioning (Hurley et al., 1995; Babiarz et al., 1998; Benoit et al., 1999b). Although our understanding of Hg and MeHg cycling in the environmental has advanced significantly in recent years, a complete understanding of Hg and MeHg speciation is lacking aside from thermodynamic predictions. Specifically, the relative role of iron/manganese oxides, dissolved organic matter (DOM), and sulfide as ligands in controlling Hg and MeHg speciation and the interaction of these ligand classes are poorly understood.

The fate of Hg introduced into a lake is expected to be linked to both transport and biogeochemical processes. Sedimentation of biogenic organic particles into the hypolimnion of stratified lakes results in an environment of high microbial activity and changing redox conditions, producing ligands that control Hg and MeHg speciation, and subsequent fate, transport, methylation, and bioavailability (Hurley et al., 1991, 1994; Benoit et al., 1999b; Babiarz et al., 2003a,b). The settling particulate organic matter is also a potentially important vector for Hg transport from the epilimnion into the hypolimnion. Microbial respiration of the organic matter produces anoxic conditions at the sediment–water interface and in the overlying hypolimnetic waters, conditions which influence the cycling of mercury prior to burial in the sediments (Hurley et al., 1994; Babiarz et al., 2003a). Anoxic conditions promote reduction of sediment Fe and Mn hydrous oxides and release of reduced Fe and Mn into the overlying water. Migration to oxic/anoxic boundaries produces Fe and Mn hydrous oxides which incorporate organic matter and inorganic oxide particles/colloids which scavenge trace metals from the aqueous phase in freshwater lakes (Taillefert et al., 2000; Davis, 1984). Specifically, Fe and Mn have large adsorption capacities the can control the concentrations of other ions and dissolved organic matter. Fe and Mn have previously been implicated to be a significant in controlling Hg and MeHg distributions (Bloom et al., 1999).

The work presented here is a subproject of the "Mercury Experiment To Assess Atmospheric Loading in Canada and the United States" (METAALICUS), a study designed to better understand the relationship between atmospheric loading of Hg and bioaccumulation in fish. We focused on investigating factors that control the fate and transport of Hg and MeHg across the sediment–water interface. We describe the Fe, Mn, and organic matter cycling in the hypolimnion of Lake 658 and whether relationships to HgT and MeHg suggest an important role of these biogeochemical cycles in controlling the fate and transport of ambient and amended Hg in this experimental lake. We focus on the ambient and lake spike(^{202}Hg, purity 90.8%) Hg and MeHg pools.

2. Site description

Lake 658 (49°43.95′ N, 93° 44.20′ W) is an 8-ha first-order boreal lake located within the Experimental Lakes Area (ELA) in northwestern Ontario (Fig. 1). Dimictic Lake 658 is separated into two basins with each having a seasonally anoxic hypolimnion (Fig. 1). The maximum depth of the west and east basins are

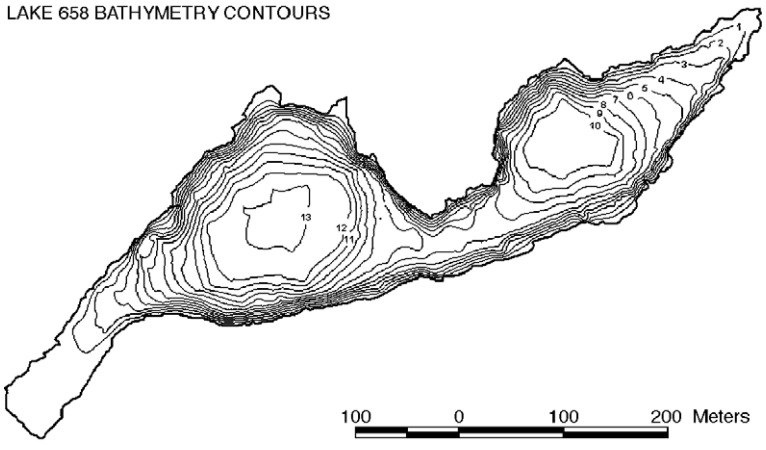

Fig. 1. Bathymetric map of Lake 658 (Middel et al., 2004).

13.4 and 10.9 m, respectively. The lake is connected to Lake 660 (Lake Winnange), and hydrological flows are measured continuously during the ice-free season. The long-term average water residence time of Lake 658 is approximately 5.5 years (Sandilands et al., 2005).

The terrestrial catchment of the watershed is dominated by jack pine (*Pinus banksiana*), black spruce (*Picea mariana*), white birch (*Betula papyrifera*), and trembling aspen (*Populous tremuloides*). Mineral soils within the watershed are thin (usually 1 m or less in depth) and discontinuous over pink Precambrian granodiorite. Soils and bedrock are typically covered with moss (*Spagnum* sp.), club moss (*Lycopodium* sp.), and lichens. Moss (*Spagnum* sp.) reaches depths greater than 0.5 m in the wetland and low-lying areas. Intermittent streamflow drains the uplands and the wetland adjacent to the lake.

3. Methods

3.1. Application of isotopic Hg to Lake 658 and its watershed

Lake 658 was dosed bi-monthly with stable ^{202}Hg nine times during each summer of 2001–2004 at a loading 4 to 5 times the annual wet deposition rate (~20 ug/m^2/year). In addition, ^{200}Hg and ^{198}Hg were applied annually at a similar loading rate to the 42-hectare upland and 2-hectare wetland portions of the lacustrine watershed, respectively. The total dose over the 2001–2003 period to each part of the ecosystem was 67 μg m^{-2} to the upland, 76 μg m^{-2} to the wetland, and 66 μg m^{-2} to the lake (Sandilands et al., 2005).

Lake spike was added every two weeks from early June until mid-October during the 2002 field season at a loading rate of 22.12 μg/m^2/year (Sandilands et al., 2005). Prior to spiking, the isotope was pre-mixed with Winnange Lake water in individual 20-L carboys. The lake spiking process involved two boats (one for each basin) powered with electric trolling motors each slowly dispensing the spike into the wake in the epilimnion (Sandilands et al., 2005). The spike solution was administered to the lake at dusk to minimize photo-reduction and evasion. The spike generally resulted in a doubling of the mercury concentration (2 to 3 ng L^{-1}) in the epilimnion of the lake (Hintelmann et al., 2005).

3.2. Sampling methods

All sampling, sample processing, and analysis for Hg and MeHg followed accepted clean techniques to minimize contamination of samples (US EPA, 1996; Olson et al., 1997; Cleckner et al., 1998). Individual water samples were collected 2, 5, 7, and 9 m from the water surface and 80, 40, 20, 10, and 5 cm from the sediment–water interface. Vertical water column profiles presented here were obtained on the day before each spike (13 days after the previous spike). Six monthly vertical profiles were collected between 31 May 2002 and 22 October 2002. Three vertical profiles are presented here: 15 July 2002, 12 August 2002, and 9 September 2002. Water column samples were obtained by using an all Teflon sampling line and weight connected to a peristaltic pump from a clean boat dedicated to mercury sampling. Filtered samples were collected from acid-cleaned in-line polyethersulfone filtration capsules rated at 0.45-um pore size (Meissner™ Filtration Products). Samples near the sediment–water interface were collected using a close interval sampler (CIS) constructed of trace-metal compatible materials that allowed us to sample at these fixed depths above the sediment–water interface (Colman, 1979; Babiarz et al., 2003a; Hurley et al., 1994).

Samples for Hg and MeHg analysis were collected in acid-cleaned Teflon bottles, double-bagged, preserved to 1% acid using 50% trace metal grade HCl, and stored at 4 °C until analysis. Major ion samples were collected in acid cleaned PTFE-lined bottles, preserved to 1% acid using 50% trace metal grade HNO_3, and stored at 4 °C until analysis. DOC samples were collected in 125 mL amber bottles and stored at 4 °C until analysis.

3.3. Analytical methods

All isotopic analyses of Hg and MeHg were performed at the state-of-the-art laboratory operated by USGS in Middleton, WI. Total mercury concentrations were determined using the bromine monochloride (BrCl) oxidation technique followed by stannous chloride (SnCl) reduction, nitrogen purging, gold-trap preconcentration, and thermal desorption (Gill and Fitzengerald, 1987). Detection was via inductively coupled plasma-mass spectrometry (ICP-MS) on a Perkin Elmer ELAN 6100 (Hintelmann et al., 2002; Babiarz et al., 2003b). MeHg was determined by distillation, aqueous phase ethylation, nitrogen purging, Carbotrap® preconcentration, thermal desorption, chromatographic separation, and ICP-MS detection (Bloom, 1989; Hintelmann et al., 1995; Hintelmann and Evans, 1997; Babiarz et al., 2003b). The analytical detection limits (three times the standard deviation of the blank) aver-

age 0.1 ng L^{-1} HgT and 0.05 ng L^{-1} MeHg. Our laboratory protocols require the re-analysis of individual samples until the relative standard deviation is within 10% and spike recoveries are within 25%.

Dissolved organic carbon (DOC) was determined using high temperature (680 °C) catalytic oxidation (Shimadzu TOC-5000) with an analytical uncertainty of ± 0.1 mg L^{-1}. Major ion composition (Fe, Mn, Ca, Mg, S, K, and Na) was determined using inductively coupled plasma-optical emission spectrometry (ICP-OES; Perkin Elmer Optima 4300 DV) with an analytical uncertainty typically under 5%. Redox potential, dissolved oxygen, temperature, pH, specific conductance were measured in the field using a multi-parameter sonde (Hydrolab™ Scout II). Total sulfide samples were preserved with sulfide anti-oxidant buffer (SAOB) and analyzed within hours using a specific ion electrode (Benoit et al., 1999a,b). The analytical detection limit for this method was 0.1 umol L^{-1}. Uncertainties in measurements of dissolved oxygen and temperature were ± 0.1 mg L^{-1} and ± 0.1 °C, respectively.

An iron speciation scheme was adopted to better understand oxidative–reductive iron cycling in Lake 658 (Taillefert et al., 2000). In this method, the particulate fraction is determined using the concentration difference between the total and filtered major ion sample. The concentration Fe(II) was determined using a modification of the 1,10-phenanthroline method (APHA, 1992). Samples were immediately fixed in the field using the colorimetric reagent. Analytical uncertainty for the spectrophotometric determination of Fe(II) was typically less than 5%. The colloidal Fe(III) fraction was calculated as the concentration difference between total Fe and Fe(II) in the filtered major ion sample, assuming that all Fe(II) in the filtrate reacts with the reagent (Taillefert et al., 2000).

4. Results and discussion

4.1. Profile development of temperature, dissolved oxygen, Fe, Mn, DOC, and sulfide

Lake 658 is a dimictic lake that thermally stratifies shortly after ice-out in April or May. Typical water column profiles for the period of summer thermal stratification are shown in Figs. 2 and 3. As the summer progresses, the thermocline eventually deepens to approximately 5 m and gradually becomes shallower in fall until thermal mixing in late October–early November. The thermocline mid-point was positioned at approximately 5 m on 12 August and 9 September profiles (Figs. 2 and 3).

Dissolved oxygen profiles in the west basin of Lake 658 show development of anoxic conditions in the hypolimnion during summer stratification. Oxygen concentrations in the epilimnion ranged from 6.45 to

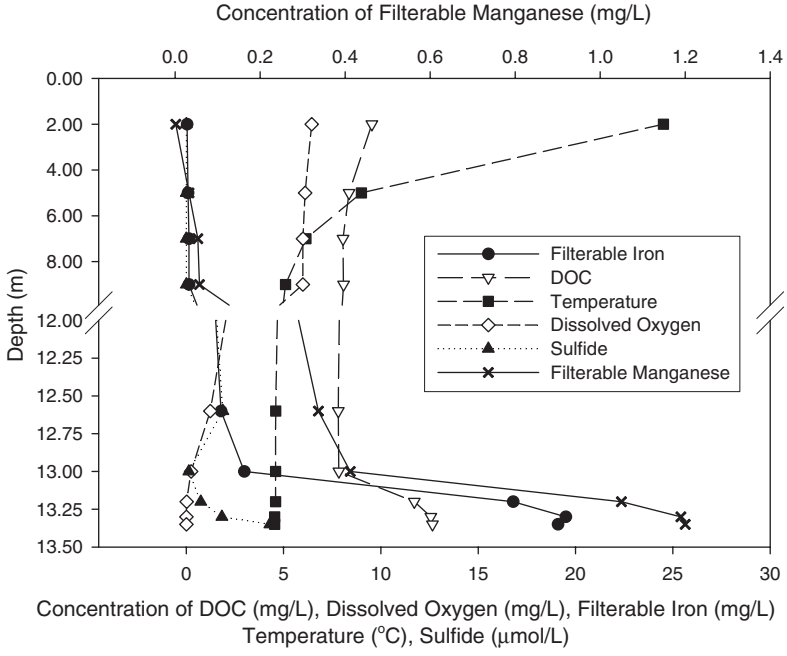

Fig. 2. Profiles of filterable iron and manganese, DOC, dissolved oxygen, sulfide and temperature in the water column of the west basin of Lake 658 on the 12 August 2002.

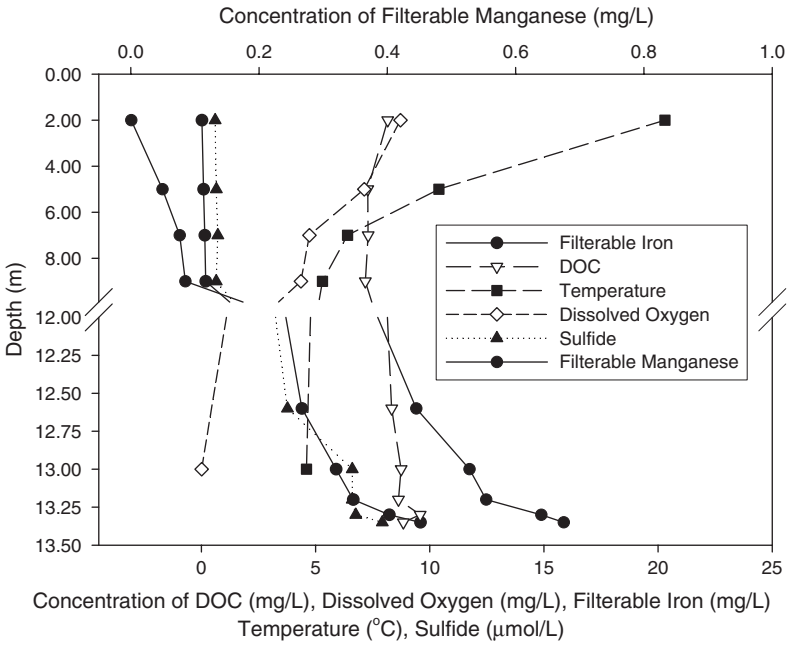

Fig. 3. Profiles of filterable iron and manganese, DOC, dissolved oxygen, sulfide and temperature in the water column of the west basin of Lake 658 on the 9 September 2002.

10.12 mg L^{-1} (77–121% of saturation) in 2002. The maximum is associated with primary production in the epilimnion. Organic particles from primary production, terrestrial transport, and resuspension of littoral sediments settle into the hypolimnion resulting in microbial respiration of the organic matter that produces anoxic conditions at the sediment–water interface and in the overlying hypolimnetic waters. The extent of anoxia in the hypolimnion increases through the late summer months (Figs. 2 and 3) until the breakdown of the thermocline in the fall resulting in rapid reoxygenation of the hypolimnion.

Hypolimnetic anoxia results in a reductive dissolution of Fe(III) and Mn(III, IV) oxide from the sediments followed by diffusion of soluble Fe(II) and Mn(II) to the overlying waters. Concentrations of Fe and Mn in the epilimnion are low and show little temporal variation. The average epilimnetic concentration of filterable Fe and Mn in 2002 were 87.3 ± 20.8 ug L^{-1} ($n=6$) and 16.4 ± 9.0 ug L^{-1} ($n=6$), respectively. The hypolimnion, on the other hand, shows enrichment in Fe and Mn (up to about 20 and 1 mg L^{-1}, respectively) near the sediment–water interface with increasing anoxia (Figs. 2 and 3). Hypolimnetic enrichment indicates that reductive mobilization occurred primarily at the sediment–water interface and that iron and manganese oxides are present within the sediments prior to the onset of anoxia.

Filterable Mn (as Mn(II)) remained in the water column longer than filterable iron (Figs. 2 and 3). This can be attributed to the higher standard potential of the Mn oxidation reaction and the slower oxidation kinetics of Mn(II) (Davison, 1993). The linear and concave shapes of the overall dissolved iron and manganese profiles near the sediment–water interface during the summer months indicate that the dominant source of dissolved Fe to the hypolimnion is reduction of Fe and Mn oxides in the sediment and diffusion to the overlying water; however, the slight convex shape near the sediment–water interface indicates that the reduction of Fe and Mn oxides associated with settling particles from redox cycling is also important in controlling the distribution of Fe and Mn in the hypolimnion (Davison, 1993; Balistrieri et al., 1992). While recycling from bottom sediments appears to be the dominant source for enrichment of the hypolimnion with Fe and Mn during summer, resuspension of littoral sediments and export from the terrestrial catchment and are likely the main net sources of Fe and Mn to the lake and the hypolimnetic sediments. Diagenesis of settling particulate Fe and Mn from these sources may augment levels of reduced Fe and Mn in the hypolimnion.

Concentration profiles for DOC are very similar to those of Fe and Mn (Figs. 2 and 3). Lake 658 is highly colored due to export of allochthonous organic matter from the surrounding watershed. The concentration of

DOC shows very little temporal variation in the epilimnion during the summer months averaging 8.64 ± 1.09 mg L^{-1} ($n=6$). On the other hand, the concentration of DOC increases significantly near the sediment–water interface in the anoxic zone. This enrichment in DOC near the sediment–water interface is often attributed to decomposition of natural organic matter associated with recently fallen particles (Tipping and Woof, 1983; Hamilton-Taylor et al., 1996; Hongve, 1997), but it may also reflect release of sediment-bound DOC associated with dissolution of Fe and Mn hydrous oxides from the sediments.

Concentration profiles for sulfide are also very similar to those of Fe and Mn (Figs. 2 and 3); however, sulfide appears in the hypolimnion after Fe and Mn become enriched. Early in the summer, sulfide is generally detectable only within 10 cm from the sediment–water interface; however, as the summer progresses and extent of anoxia increases, sulfide migrates higher in the water column. On the 12 August 2002, detectable sulfide ranged from 0.14–4.29 μmol L^{-1}, and was localized within 1 m of the sediment–water interface (Fig. 2). On 9 September 2002, detectable sulfide ranged from 0.14–7.92 μmol L^{-1}, and sulfide had migrated to 6 m above the sediment–water interface (Fig. 3).

Sulfide concentrations are not sufficiently high to control Fe(II) solubility and restrict Fe(II) release from the sediments. However, the concentrations of Fe(II) and sulfide in the hypolimnion during late summer were high enough to cause precipitation of FeS assuming the log $K_{sp}=-2.9\pm0.1$ for fresh FeS (Berner, 1967; Schoonen and Barnes, 1988; Balistrieri et al., 1992). This formation of FeS in late summer is consistent with visual observations of black particulates and colloids from samples collected near the sediment–water interface. The precipitation of Mn sulfide phases was not thermodynamically favorable in the hypolimnion of Lake 658. Carbonate was also relatively low in the water column (S. Chadwick, unpublished data); therefore, precipitation of $FeCO_3$ (siderite) and $MnCO_3$ (rhodochrosite) is insignificant.

4.2. Relationship between Fe, Mn, and DOC

The distribution of DOC is correlated closely with the distribution of filterable iron ([Filterable Fe] = 3.305 ± 0.172[DOC] − 22.82 ± 1.681, $r^2=0.966$, $n=15$, $p<0.001$) and manganese ([Filterable Mn] = 0.162 ± 0.00867[DOC] − 0.872 ± 0.0849, $r^2=0.964$, $n=15$, $p<0.001$). This relationship is not surprising for two reasons. First, Mn and Fe hydrous oxides can serve as electron acceptors in the biological oxidation of organic matter. Thus, settling of particulate organic matter into the hypolimnion leads to release of Fe and Mn from sediments and may promote release of sediment-bound DOC. Through this pathway, organic matter can dictate the chemical and physical form of Fe and Mn (Balistrieri et al., 1992). Second, microscopic investigations have shown that hydrous oxides and high molecular weight natural organic matter (NOM) can form intimate structures (Fortin et al., 1993; Taillefert et al., 2000) at well-defined redox boundaries that can scavenge trace metals during surface complexation and occlusion (Laxen, 1985; Taillefert et al., 2000). These Fe oxide–DOM aggregates were visually observed on particulates collected from the hypolimnion of Lake 658. Dissolution of these aggregates in the anoxic hypolimnion increases the concentrations of both Fe and DOC.

Due to the differences in standard potential, rates of diffusion, and kinetics of oxidation, differences in the water column distribution of Fe and Mn are expected. However, there was also a very strong relationship between filterable Fe and Mn in the water column of Lake 658 ([Filterable Mn] = 0.0489 ± 0.00140[Filter- 0.00140[Filterable Fe] + 0.251 ± 0.0158, $r^2=0.986$, $n=15$, $p<0.001$). This reflects the reduction of Fe and Mn hydrous oxides in the sediments as a common in-lake source of hypolimnetic Fe(II) and Mn(II) and also suggests that the watershed exports a fairly consistent mass ratio of Mn : Fe of 0.05 to the lake.

4.3. Role of reactive iron transport

A model for describing reactive transport of Fe and Mn was originally proposed by Davison (1985). In this conceptual model, Fe and Mn oxides are generated at the oxic–anoxic boundary due to oxidation, and these oxides are vertically transported by diffusion and settling. The result of this process is a generation of a particulate hydrous oxide peak at this boundary above the reduced portion of the concentration profile. The position and magnitude of this peak are dependent on the standard potential for oxidation of the metal and the kinetics of oxidation.

Since the concentration of Fe was generally an order of magnitude greater than the concentration of Mn in the hypolimnion, this conceptual model was applied to the Fe cycling in Lake 658 using an iron speciation scheme adopted by Taillefert et al. (2000), Taillefert and Gaillard (2002). Concentration profiles for particulate Fe, colloidal Fe(II), Fe(II), and dissolved oxygen for the 12 August 2002 are presented in Fig. 4. As in the

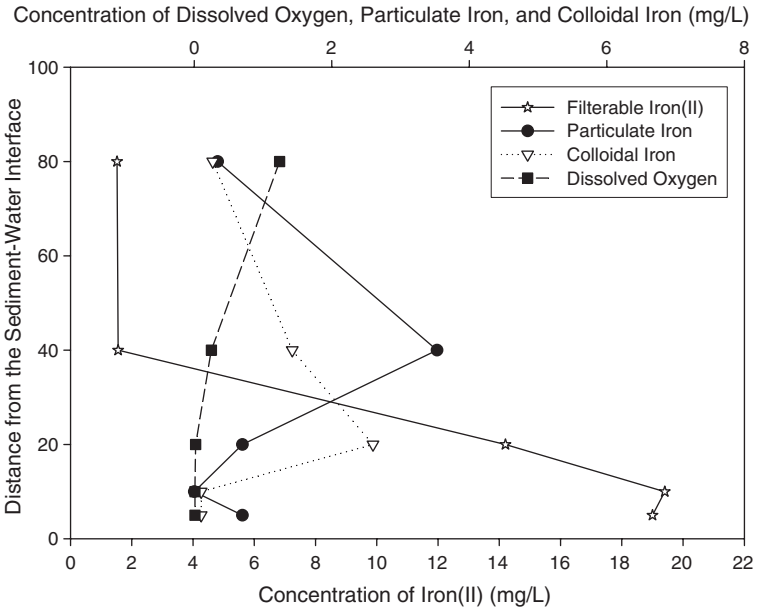

Fig. 4. Profile of dissolved oxygen and iron species in the water column near the sediment–water interface of the west basin of Lake 658 on the 12 August 2002.

conceptual model, a well-defined particulate Fe peak is present at the oxic–anoxic transition in the hypolimnion. This particulate Fe peak settles and persists in the anoxic portion of the hypolimnion. As the particulate Fe is reduced, the Fe becomes colloidal in size. This is consistent with observation of a colloidal Fe(III) peak present further into the anoxic zone (Fig. 4).

Our iron speciation results suggest a persistence of Fe(III) oxide particles in anoxic environments despite thermodynamic predictions as reported previously (Taillefert et al., 2000). Apparently, the rate of settling of particulate Fe is faster than the rate of reduction and dissolution. If DOM and Fe form complex aggregates at the oxic–anoxic transition, particulate Fe could be a vector for transport of DOC to the sediment–water interface.

4.4. Concentration profiles of the ambient and lake spike pools of Hg and MeHg

Concentration profiles for the ambient and lake spike pools of HgT and MeHg on the 15 July 2002, 12 August 2002, and 9 September 2002 are presented in Figs. 5–7. Added isotopic mercury in the filtered phase remained largely in the epilimnion until the thermocline broke down in the fall (Babiarz et al., 2003a). The concentration of filtered ambient and lake spike HgT in the epilimnion ranged from 2.25–2.63 and 0.63–0.94 ng L^{-1}, respectively, from 15 July 2002 to 9 September 2002. Transport of isotopic mercury from the epilimnion to the hypolimnion was primarily through settling particulate matter (Babiarz et al., 2003a). Diagenesis of these recently-fallen particles resulted in elevated filterable ambient and lake spike HgT near the sediment–water interface (Figs. 5–7). Filtered ambient and lake spike HgT near the sediment–water interface ranged from 1.53–8.59 and 0.27–2.43 ng L^{-1}, respectively, in the filtered phase from 15 July 2002 to 9 September 2002. Ambient HgT profiles were very similar to lake spike HgT profiles in the hypolimnion indicating similar recycling at or near the sediment–water interface (Figs. 5–7). The historic pool of Hg from the sediments was of minor importance. There does not appear to be a large influence of porewater release from deeper sediments or these profiles would be expected to diverge.

Methylated Hg from the lake spike was first noted in settling particulate matter two weeks after the initial spike in 2001 (Babiarz et al., 2003a). Ambient and lake spike MeHg concentrations in the epilimnion ranged from 0.08–0.20 and 0.01–0.02 ng L^{-1}, respectively, in the filtered phase from 15 July 2002 to 9 September 2002. The MeHg profiles show a low concentration of MeHg in the upper water column with increasing concentrations near the sediment–water interface (Figs. 5–7). MeHg was strongly associated with particles that delivered MeHg to the sediment–water interface (Babiarz et al., 2003a) resulting in enhanced filtered phase MeHg concentrations following diagenesis of these particles in the hypolimnion (Figs. 5–7). Filtered ambient and lake spike MeHg near the sediment–water

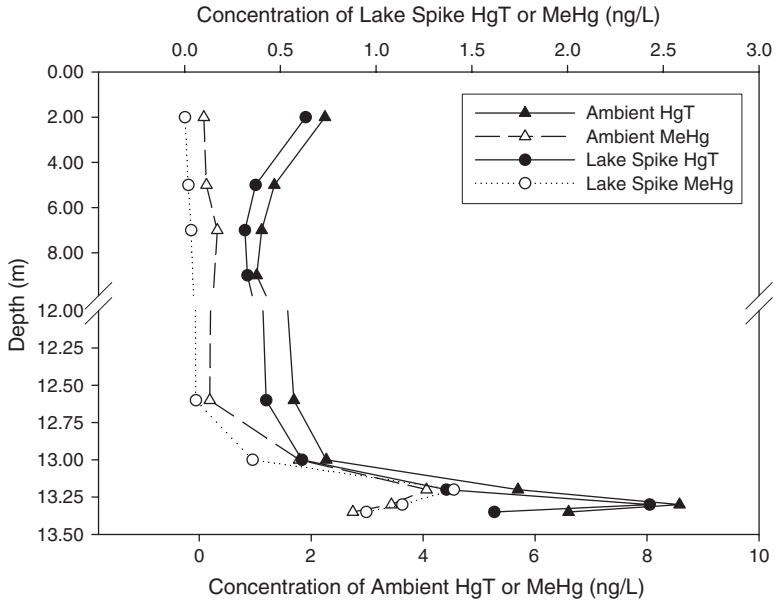

Fig. 5. Profiles of filtered ambient and lake spike HgT and MeHg in the water column of the west basin of Lake 658 on the 15 July 2002.

interface (taken from the CIS) ranged from 0.19–4.06 and 0.06–1.41 ng L^{-1}, respectively, in the filtered phase from 15 July 2002 to 9 September 2002. Similar to HgT profiles, ambient MeHg profiles were also very similar to lake spike MeHg profiles again indicating that deep porewater release of MeHg is probably not important (Figs. 5–7).

The fraction of total mercury as methylmercury in the water column for both the ambient and lake spike pools on 15 July 2002 and 9 September 2002 are presented in Fig. 8. In the epilimnion, the fraction as methylmercury was slightly greater for the ambient pool than the lake spike pool. However, in the hypolimnion, the fraction of total mercury as methylmercury is usually greater for the lake spike pool than the ambient pool (Fig. 8). This observation suggests that the lake spike may be more reactive to methylation than the ambient pool. We cannot, at this point, deter-

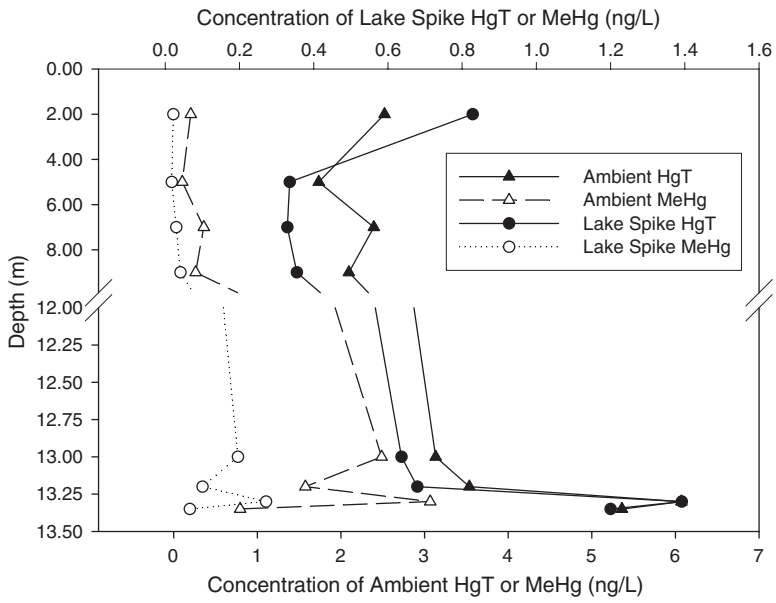

Fig. 6. Profiles of filtered ambient and lake spike HgT and MeHg in the water column of the west basin of Lake 658 on the 12 August 2002.

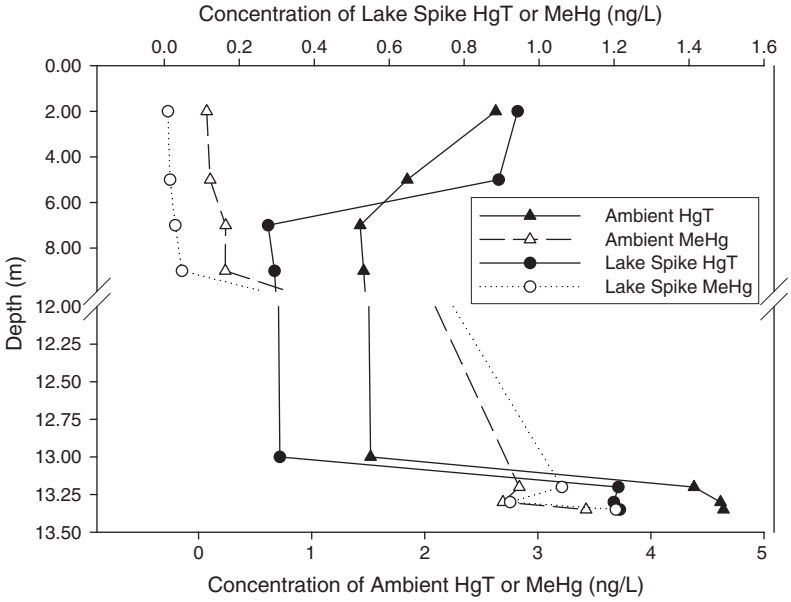

Fig. 7. Profiles of filtered ambient and lake spike HgT and MeHg in the water column of the west basin of Lake 658 on the 9 September 2002.

mine whether MeHg in the hypolimnion is derived from diagenesis of settled particles or from direct methylation in the hypolimnion. However, our CIS sampling shows that very little Hg(II) is present in the filtered phase in the zone directly above the sediment–water interface. The MeHg profile likely reflects production by methylation in the hypolimnion combined with scavenging by Fe-organic particles at the oxic–anoxic boundary that acts to retain MeHg in the hypolimnion.

4.5. Relationship between the ambient and lake spike pools for HgT and MeHg

There is a very strong relationship ([Lake Spike] = 0.250 ± 0.0147[Ambient] $- 0.0934 \pm 0.0594$, $r^2 = 0.920$, $n = 27$, $p < 0.001$) between the lake spike HgT and ambient HgT. Similarly, there is a very strong relationship ([Lake Spike] $= 0.345 \pm 0.0140$[Ambient] $- 0.0594 \pm 0.0280$, $r^2 = 0.967$, $n = 23$, $p < 0.001$) between the lake spike MeHg and ambient MeHg. These two strong rela-

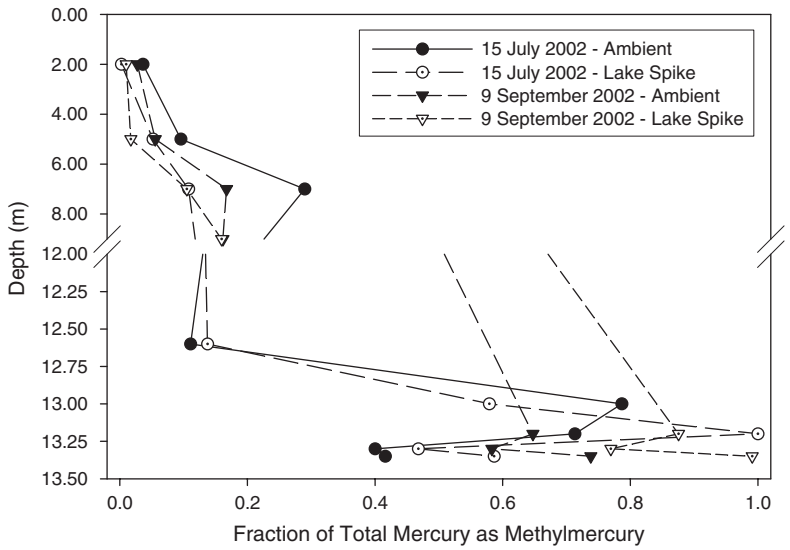

Fig. 8. Profiles of the fraction of HgT as MeHg for the ambient and lake spike pools in the water column of the west basin of Lake 658 on the 15 July 2002 and 9 September 2002.

tionships indicate that similar biogeochemical processes are controlling the temporal and spatial distribution of the lake spike and ambient pools of HgT and MeHg in the water column. The epilimnetic samples have the greatest variability in both relationships; however, this variability is expected since the epilimnion was the portion of the lake periodically amended with stable inorganic ^{202}Hg.

4.6. Relationship between DOC and the ambient and lake spike pools of HgT

Dissolved organic carbon has long been implicated as a dominant ligand controlling the fate and transport of Hg and MeHg in aquatic environments (Andren and Harriss, 1975; Babiarz et al., 2001; Amirbahman et al., 2002; Haitzer et al., 2002). A similar positive relationship was found between DOC and the ambient and lake spike pools of filterable HgT. The relationship between filterable ambient HgT and DOC ([Ambient HgT] = 0.740 ± 0.179[DOC] $- 3.144 \pm 1.636$, $r^2 = 0.406$, $n = 27$, $p < 0.001$) is slightly than stronger the relationship between filterable lake spike HgT and DOC ([Lake Spike HgT] = 0.169 ± 0.0501[DOC] $- 0.740 \pm 0.457$, $r^2 = 0.314$, $n = 27$, $p = 0.002$); however, this difference is likely not statistically significant. On the other hand, the concentration of Hg resulting from the lake spike is independent of any addition of DOC from external sources, while the ambient Hg is the result of co-transport of DOC and Hg from the watershed and simultaneous release of DOC and Hg from lake particulate matter. This difference in loading may explain the weaker relationship between lake spike HgT and DOC versus ambient HgT and DOC. The correlation between lake spike Hg and DOC indicates that Hg associates rapidly with natural organic matter (NOM), and it remains distributed with NOM in the water column after particle diagenesis.

The relation between HgT and DOC further suggests that organic carbon plays an important role in the transport of HgT in the hypolimnion. Moreover, the concentration of HgT and MeHg in the hypolimnion is not controlled solely by the redox cycling of Fe and Mn. The variability in the HgT : DOC relation as compared to the Fe : DOC relation indicates that filterable HgT is sensitive to processes that are less important for Fe(II). For example, the speciation of Hg(II) is likely influenced more than Fe(II) by metal-binding organic ligands and sulfide produced in the hypolimnion. Changes in speciation could influence the reactivity and aqueous–solid phase partitioning of Hg(II), causing variability in the HgT–DOC relationship. In addition, methylation causes changes in the Hg(II)–MeHg ratios, representing another influence on filterable HgT but not on filterable Fe.

There was a very weak relationship ($r^2_{\text{Ambient}} = 0.077$; $r^2_{\text{Lake Spike}} = 0.072$) between MeHg and DOC for the Lake 658 profiles examined (S. Chadwick, unpublished data). Several factors may account for the lack of a strong relationship between the concentrations of filterable MeHg and DOC. The distributions of HgT and MeHg are controlled, in part, by different mechanisms in the hypolimnion. The HgT and DOC increase with depth is likely linked to diagenesis of newly-fallen organic particles, while the distribution of MeHg is also controlled by rates of methylation and demethylation. Similarly to Hg(II), scavenging by Fe-organic particles probably enhances retention of MeHg in the hypolimnion, but the methylation–demethylation cycle is another controlling process. Little non-methyl Hg is present near the sediment–water interface during maximum stratification. Additionally, strong metal-binding ligands (e.g., sulfide) influence the speciation and reactivity of MeHg and the bioavailability of Hg(II) for methylation (Benoit et al., 1999b). For example, high DOC concentrations near the sediment–water interface may reduce the bioavailability of Hg to methylating bacteria due to the large macromolecular size of DOM and strong intrinsic binding to DOM (Miskimmin et al., 1992; Ravichandran, 2004).

4.7. Implications of Fe/Mn/DOC cycling on the biogeochemical cycling of Hg and MeHg

Since DOM is a controlling variable in the distribution of Hg and MeHg in the water column of Lake 658, it is likely that Fe and Mn have an indirect influence in controlling the fate and transport of Hg and MeHg in the hypolimnion. This influence may occur through binding of Hg and MeHg to organic matter associated with Fe and Mn hydrous oxides, through Fe and Mn serving as electron acceptors in the decomposition of particulate organic matter containing Hg(II) and MeHg delivered to the sediment–water interface, and/or by aggregation of DOC–Hg/MeHg species into colloids and particulates at a well-defined redox boundary.

Iron speciation data suggests that of Fe(III) oxide particles persist in anoxic zone of Lake 658 despite thermodynamic predictions (Fig. 4). If Hg is strongly associated with DOC in the water column, and Fe has a controlling influence on the transport of DOC through the generation of DOC–Fe colloids and particulates, Fe is important delivery mechanism of DOC–Hg com-

plexes to the sediment–water interface. This has obvious implications on the long-term fate, transport, and methylation of the amended isotope.

In addition, recent research has shown that Fe can influence on the methylation potential of Hg by controlling the sulfide activity (Mehrotra et al., 2003). This dataset suggests that Fe(II) has a controlling influence on sulfide activity in the hypolimnion of Lake 658 through the precipitation of FeS. Consideration of the role of Fe(II) in the formation of neutral Hg-sulfide complexes (Benoit et al., 1999b) may be important in explaining methylation rates and MeHg distributions in the hypolimnion of Lake 658.

Acknowledgements

This manuscript is contribution #22 from METAALICUS. The presented work was performed at the Experimental Lakes Area operated by the Department of Fisheries and Oceans in Canada. The authors express their gratitude to Moore, Tate, Trinko, Sandilands, and Page for their help with field work, analysis, and sampling design. The authors further express their gratitude to Krabbenhoft, Olson, Olund, and DeWild for the use of clean room facilities and the ICP-MS at the USGS office (Middleton, WI). This work was supported by the University of Wisconsin Water Resources Institute through the USGS-NIWR Competitive Grants Program (Project 00HQGR0094), Wisconsin Department of Natural Resources (Project No. NMC00000171), Wisconsin Focus on Energy (Project No. 4900-02-03), and the Electric Power Research Institute (Project No. EP-P6174/C3124).

References

American Public Health Association (APHA). Phenanthroline method for Fe (3500-D). In: Greenberb EA, Clesceri LS, Eatson AD, editors. Standard methods for examination of water and wastewater. 18th edition; 1992. p. 66–8.

Amirbahman A, Reid AL, Haines TA, Kahl JS, Arnold C. Association of methylmercury with dissolved humic acids. Environ Sci Technol 2002;36:690–5.

Andren A, Harriss R. Observations on the association between mercury and organic matter dissolved in natural waters. Geochim Cosmochim Acta 1975;39:1253–7.

Babiarz CL, Hurley JP, Benoit JM, Shafer MM, Andren AW, Webb DA. Seasonal influences on partitioning and transport of total and methylmercury in rivers from contrasting watersheds. Biogeochemistry 1998;41:237–57.

Babiarz CL, Hurley JP, Hoffmann SR, Andren AW, Shafer MM, Armostrong DE. Partitioning of total mercury and methylmercury to the colloidal phase in freshwaters. Environ Sci Technol 2001; 35:4773–82.

Babiarz CL, Hurley JP, Krabbenhoft DP, Trinko TR, Tate M, Chadwick SP, et al. A hypolimnetic mass balance of mercury from a dimictic lake: results from the METAALICUS project. J Phys IV 2003a;107(1):83–6.

Babiarz CL, Hurley JP, Krabbenhoft DP, Gilmour C, Branfireun BA. Application of ultrafiltration and stable isotopic amendments to field studies of mercury partitioning to filterable carbon in lake water and overland runoff. Sci Total Environ 2003b;304(1–3): 295–303.

Balistrieri LS, Murray JW, Paul P. The cycling of iron and manganese in the water column of Lake Sammamish, Washington. Limnol Oceanogr 1992;37(3):510–28.

Benoit JM, Mason RP, Gilmour CC. Estimation of mercury-sulfide speciation in sediment pore waters using octanol–water partitioning and implications for availability to methylating bacteria. Environ Toxicol Chem 1999a;18:2138–41.

Benoit JM, Gilmour CC, Mason RP, Heyes A. Sulfide controls on mercury speciation and bioavailability to methylating bacteria in sediment pore waters. Environ Sci Technol 1999b;33:951–7.

Benoit JM, Gilmour CC, Mason RP. Aspects of bioavailability of mercury for methylation in pure cultures of *Desulfobulbus propionicus* (1pr3). Appl Environ Microbiol 2001a;67:51–8.

Benoit JM, Gilmour CC, Mason RP. The influence of sulfide on solid phase mercury bioavailability for methylation by pure cultures of *Desulfobulbus propionicus* (1pr3). Environ Sci Technol 2001b; 35:127–32.

Berner RA. Thermodynamic stability of sedimentary iron sulfide. Am J Sci 1967;265:773–85.

Bloom NS. Determination of pictogram levels of methylmercury by aqueous-phase ethylation, followed by cryogenic gas chromatography with cold vapor atomic fluorescence detection. Can J Fish Aquat Sci 1989;46:1131–40.

Bloom NS, Gill GA, Cappellino S, Dobbs C, Driscoll C, Mason RP, et al. Speciation and cycling of mercury in Lavaca Bay, Texas, sediments. Environ Sci Technol 1999;33:7–13.

Cleckner LB, Garrison PJ, Hurley JP, Olson ML, Krabbenhoft DP. Trophic transfer of methylmercury in the northern Florida Everglades. Biogeochemistry 1998;40:347–61.

Colman, JA. Measurement of eddy diffusivity and solute transport through the near-sediment boundary layer of ice-covered lakes, using Radon-222. Ph.D. Thesis. University of Wisconsin-Madison; 1979.

Compeau GC, Bartha R. Sulfate-reducing bacteria — principle methylators of mercury in anoxic estuarine sediment. Appl Environ Microbiol 1985;50:498–502.

Davis JA. Complexation of trace metals by adsorbed organic matter. Geochim Cosmochim Acta 1984;48:679–91.

Davison W. Conceptual model for transport at a redox boundary. In: Stumm W, editor. Chemical processes in lakes. Wiley-Interscience; 1985.

Davison W. Iron and manganese in lakes. Earth Sci Rev 1993;34: 119–63.

Fortin D, Leppard GG, Tessier A. Characteristics of lacustrine diagenic iron oxyhydroxides. Geochim Cosmochim Acta 1993;57: 4391–404.

Gill GA, Fitzengerald WF. Picomolar mercury measurements in seawater and other materials using stannous chloride reduction and two-stage gold amalgamation with gas-phase detection. Mar Chem 1987;20:227–43.

Gilmour CC, Henry EA, Mitchell R. Sulfate simulation of mercury methylation in freshwater sediments. Environ Sci Technol 1992; 26:2281–7.

Haitzer M, Aiken GR, Ryan NJ. Binding of mercury(II) to dissolved organic matter: the role of the mercury-to-DOM concentration ratio. Environ Sci Technol 2002;36:3564–70.

Hamilton-Taylor J, Davison W, Morfett K. The biogeochemical cycling of Zn, Cu, Fe, Mn, and dissolved organic C in a seasonally anoxic lake. Limnol Oceanogr 1996;41(3):408–18.

Hintelmann H, Evans RD. Application of stable isotopes in environmental tracer studies: measurement of monomethylmercury (CH_3Hg^+) by isotope dilution ICP-MS and detection of species transformation. Fresenius' J Anal Chem 1997;358:378–85.

Hintelmann H, Evans RD, Villeneuve JY. Measurement of mercury methylation in sediment by using enriched stable mercury isotopes combined with methylmercury determination by gas-chromatography inductively-coupled plasma mass-spectrometry. J Anal At Spectrom 1995;10:619–24.

Hintelmann H, Harris R, Heyes A, Hurley JP, Kelly CA, Krabbenhoft DP, et al. Reactivity and mobility of new and old mercury deposition in a Boreal forest ecosystem during the first year of the METAALICUS study. Environ Sci Technol 2002;36:5034–40.

Hintelmann H, Ogrinc N, Sandilands K, Dimock B. Distribution of inorganic and methylmercury in METAALICUS Lake 658 after addition of stable isotopes. In: Horvat H, Ogrinc N, Faganeli J, Kotnik, editors. JRMZ: materials and geoenvironment, Part 2; 2005. p. 1064–5.

Hongve D. Cycling of iron, manganese, and phosphorus in a meromictic lake. Limnol Oceanogr 1997;42(4):635–47.

Hurley JP, Watras CJ, Bloom NS. Mercury cycling in a northern Wisconsin seepage lake—the role of particulate matter in vertical transport. Water Air Soil Pollut 1991;56:543–51.

Hurley JP, Krabbenhoft DP, Babiarz CL, Andren AW. Cycling of mercury across the sediment–water interface in seepage lakes. Environmental chemistry of lakes and reservoirs. Amer Chem Soc, Washington; 1994. p. 425–49.

Hurley JP, Benoit JM, Babiarz CL, Shafer MM, Andren AW, Sullivan JR, et al. Influences of watershed characteristics on mercury levels in Wisconsin Rivers. Environ Sci Technol 1995;29:1867–75.

Laxen DPH. Trace metal adsorption/co-precipitation on hydrous ferric oxide under realistic conditions: the role of humic substances. Water Res 1985;19:1229–36.

Mehrotra AS, Horne AJ, Sedlak DL. Reduction of net mercury methylation by iron in *Desulfobulbus propionicus* (1pr3) cultures: implications for engineered wetlands. Environ Sci Technol 2003; 37:3018–23.

Middel, T, Flavelle, L, Sandilands, K. Lake 658 bathymetry. Ontario Ministry of Natural Resources. Department of Fisheries and Oceans-Canada 2004.

Miskimmin BM, Rudd JM, Kelly CA. Influence of dissolved organic carbon, pH, and microbial respiration rates on mercury methylation and demethylation in lake water. Can J Fish Aquat Sci 1992; 49:17–22.

Olson ML, Cleckner LB, Hurley JP, Krabbenhoft DP, Heelan TW. Resolution of matrix effects on analysis of total and methylmercury in aqueous samples from the Florida Everglades. Fresenius' J Anal Chem 1997;358:392–6.

Ravichandran M. Interactions between Hg and dissolved organic matter — a review. Chemosphere 2004;55(3):319–31.

Sandilands KA, Rudd JWM, Kelly CA, Hintelmann H, Gilmour CC, Tate MT. Application of enriched stable mercury isotopes to the Lake 658 watershed for the METAALICUS project, at the Experimental Lakes Area, northwestern Ontario, Canada. Can Tech Rep Fish Aquat Sci 2005;2597. viii+48 p.

Schoonen MAA, Barnes HL. An approximation of the second dissociation constant for H_2S. Geochim Cosmochim Acta 1988;54: 903–8.

Taillefert M, Gaillard JF. Reactive transport modeling of trace elements in the water column of a stratified lake: iron cycling and metal scavenging. J Hydrol 2002;256:16–34.

Taillefert M, Lienemann CP, Gaillard JF, Perret D. Speciation, reactivity, and cycling of Fe and Pb in a meromictic lake. Geochem Cosmochim Acta 2000;64(2):163–9.

Tipping E, Woof C. Elevated concentrations of humic substances in a seasonally anoxic hypolimnion: evidence of co-accumulation with iron. Arch Hydrobiol 1983;115:59–70.

US Environmental Protection Agency. Method for sampling ambient water for determination of metals at EPA ambient criteria levels EPA 821-R-96-011. Office of Water, Washington DC: US EPA; 1996.

Watras CJ, Morrison KA, Bloom NS. Chemical correlates of Hg and methyl-Hg in northern Wisconsin lake waters under ice cover. Water Air Soil Pollut 1995;84:253–67.